THE INFRARED SPECTROGRAPH[1] (IRS) ON THE SPITZER SPACE TELESCOPE

J. R. Houck,[2] T. L. Roellig,[3] J. van Cleve,[4] W. J. Forrest,[5] T. Herter,[2] C. R. Lawrence,[6] K. Matthews,[7]
H. J. Reitsema,[4] B. T. Soifer,[8] D. M. Watson,[5] D. Weedman,[2] M. Huisjen,[4] J. Troeltzsch,[4]
D. J. Barry,[2] J. Bernard-Salas,[2] C. E. Blacken,[2] B. R. Brandl,[9] V. Charmandaris,[2,10] D. Devost,[2]
G. E. Gull,[2] P. Hall,[2] C. P. Henderson,[2] S. J. U. Higdon,[2] B. E. Pirger,[2] J. Schoenwald,[2]
G. C. Sloan,[2] K. I. Uchida,[2] P. N. Appleton,[8] L. Armus,[8] M. J. Burgdorf,[8] S. B. Fajardo-Acosta,[8]
C. J. Grillmair,[8] J. G. Ingalls,[8] P. W. Morris,[8,11] AND H. I. Teplitz[8]
Received 2004 March 30; accepted 2004 June 3

ABSTRACT

The Infrared Spectrograph (IRS) is one of three science instruments on the Spitzer Space Telescope. The IRS comprises four separate spectrograph modules covering the wavelength range from 5.3 to 38 μm with spectral resolutions, $R = \lambda/\Delta\lambda \approx 90$ and 600, and it was optimized to take full advantage of the very low background in the space environment. The IRS is performing at or better than the prelaunch predictions. An autonomous target acquisition capability enables the IRS to locate the mid-infrared centroid of a source, providing the information so that the spacecraft can accurately offset that centroid to a selected slit. This feature is particularly useful when taking spectra of sources with poorly known coordinates. An automated data-reduction pipeline has been developed at the Spitzer Science Center.

Subject headings: infrared: general — instrumentation: spectrographs — space vehicles: instruments

1. INTRODUCTION

The design of the IRS was driven by the objective of maximizing sensitivity given the 85 cm aperture of the Spitzer Space Telescope (Werner et al. 2004) and the then-available detectors. Dividing the optical trains of the IRS into four separate spectrographs substantially reduced the complexity and overall cost of the system. The result is four separate modules, known by their wavelength coverage and resolution as Short-Low (SL), Short-High (SH), Long-Low (LL), and Long-High (LH). The slit widths are set to $\lambda_{max}/85$ cm, where λ_{max} is the longest wavelength for the module. Further in the geometric limit the monochromatic slit image covers two pixels. Two Si : As detectors, 128×128 pixels in size, collect the light in the SL and SH modules, while two Si : Sb detectors of the same number of pixels are used in the LL and LH modules. In addition to its spectrographs, the IRS contains two peak-up imaging fields, which are built into the SL module and have bandpasses centered at 16 μm ("blue") and 22 μm ("red"). A picture of IRS is presented in Figure 1, and Table 1 gives the parameters of each module.

The two long-slit low-resolution modules were designed for optimum sensitivity to dust features in the local and distant universe and are effectively limited in sensitivity by the zodiacal and/or Galactic backgrounds. The two cross-dispersed high-resolution echelle modules were designed to achieve the highest possible resolution for the given array dimensions, and they were optimized for sensitivity to emission lines.

In the following sections we describe the instrument, its operation and calibration, and the reduction of its data using the pipeline developed at the Spitzer Science Center (SSC). The Spitzer Observer's Manual (SOM) provides a more thorough discussion, and it is updated frequently.[12]

2. DESIGN, MANUFACTURE, AND GROUND TESTING

The IRS contains no moving parts. The diamond-machined optics are bolted directly to the precision-machined module housings, and all are constructed of aluminum so that the assembled modules retain their focus and alignment from room temperature to their operating temperature near 1.8 K without any further adjustment. The focal plane assemblies are equipped with custom plates to interface with the module housing and account for the individual dimensions and locations of the arrays. Each module contains two flood-illuminating stimulators to monitor the performance of the arrays.

The low-resolution modules each contain two subslits, one for the first-order spectrum and one for the second-order spectrum. When a source is in the subslit for the second order, a short piece of the first order appears on the array; this "bonus" order improves the overlap between the first and second orders. The high-resolution modules are cross dispersed so that 10 orders (11–20) fall on the array.

The modules were extensively tested at operating temperature at Ball Aerospace (Houck et al. 2000). Light from external sources passed through the Dewar window and a series

[1] The IRS was a collaborative venture between Cornell University and Ball Aerospace Corporation funded by NASA through the Jet Propulsion Laboratory and the Ames Research Center.

[2] Astronomy Department, Cornell University, Ithaca, NY 14853-6801; jrh13@cornell.edu.

[3] NASA Ames Research Center, MS 245-6, Moffett Field, CA 94035-1000.

[4] Ball Aerospace and Technologies Corporation, 1600 Commerce Street, Boulder, CO 80301.

[5] Department of Physics and Astronomy, University of Rochester, Rochester, NY 14627.

[6] Jet Propulsion Laboratory, California Institute of Technology, MC 169-327, Pasadena, CA 91125.

[7] Palomar Observatory, California Institute of Technology, Pasadena, CA 91125.

[8] Spitzer Science Center, California Institute of Technology, MC 220-6, Pasadena, CA 91125.

[9] Leiden University, 2300 RA Leiden, Netherlands.

[10] Chercheur Associé, Observatoire de Paris, F-75014 Paris, France.

[11] NASA Herschel Science Center, IPAC/Caltech, MC 100-22, Pasadena, CA 91125.

[12] See http://ssc.spitzer.caltech.edu/documents/SOM/ for the most current version of the SOM.
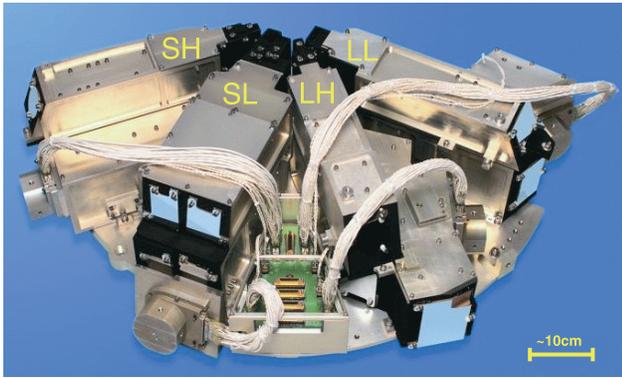
FIG. 1.—Infrared Spectrograph on *Spitzer*. The four IRS modules, SH, SL (which includes the peak-up cameras), LH, and LL are marked. A schematic of the location of the spectrograph slits on the *Spitzer* focal plane is presented in Fig. 2 of Werner et al. (2004).

of neutral density filters at liquid N_2 and He temperatures. An external optical system projected both point and extended images from either a blackbody or a monochromator onto each slit or subslit. These tests verified the resolution, internal focus, and alignment, as well as the correct centering of the spectrum on the arrays. From the beginning of testing through integration and launch, the focus and alignment of the modules has remained constant on a scale of one-tenth of a pixel. The monochromator tests allowed us to map the wavelength positions roughly on the arrays in preparation for flight.

Uncertainties in the transmission of the neutral-density filter stacks prevented a useful determination of the overall sensitivities prior to launch. Instead, the sensitivities of the modules were predicted by an analytic model of the system. Extensive observations using a prototype of the SH module at the Hale 5 m telescope verified the procedures used in the sensitivity predictions to the 20% level (van Cleve et al. 1998; Smith & Houck 2001).

When the IRS is operating, all four of its detector arrays are clocked simultaneously, but it is only possible to capture data from one array at a time. Two techniques are used in data collection, the double-correlated sampling (DCS mode) and raw data collection (Raw mode, or "sample up the ramp"). Science data are collected in Raw mode, while peak-up employs DCS. In DCS mode following an initial series of bias boost and reset frames, each pixel is sampled, and then after a number of nondestructive spins through the array each pixel is sampled again via a destructive read and the difference

between the two samples is stored as an 128×128 pixel image. In the Raw mode after the same initial bias boost, reset frames, and first sampling of pixels there are a number of spin frames followed by a nondestructive read. This pattern is repeated *n* times. When all pixels are sampled again the result is a $128 \times 128 \times n$ cube, where *n* is the number of nondestructive reads, and the values are $n = 4$, 8, or 16. A final 128×128 image is created by calculating the signal slope of each pixel of the Raw cube.

3. IN-FLIGHT OPERATION AND CALIBRATION

Mapping the relative positions of each field of view and the spacecraft's Pointing Calibration Reference Sensor (PCRS) was the most critical step of the in-orbit checkout (IOC) phase. The positions must be measured to an accuracy of better than 0″14 radial (0″28 for the long-wavelength modules) to meet the 5% radiometric requirements. The positions were measured iteratively, starting with ground-based estimates and proceeding successively through ultracoarse, coarse, and fine focal plane surveys. Combined with the determination of the focus between the telescope and the slits, this process took place over nearly six of the eight weeks of the IOC period. The estimated uncertainties in the final measured positions of the slits and the peak-up arrays are better than the requirements in all cases, ranging from 0″09 to 0″12.

Our knowledge of the internal focus and optical calibration of the spectral orders were updated in-flight using a combination of photometric standard stars and emission line objects. The widths of the orders were derived from the zodiacal light at maximum intensity, while order curvatures, tilts, and wavelength solutions were rederived from spectral maps of emission line stars such as P Cygni and planetary nebulae such as NGC 6543, NGC 7027, and SMP 083. Figure 2 presents the hydrogen recombination spectrum of the Be star γ Cas, which provides a good check of the wavelength calibration for SH.

Flat-fielding and spectrophotometric calibration are determined from mapping and staring observations of well-known standards, including ξ Dra (HR 6688, K2 III), HR 7310 (G9 III), and HR 6606 (G9 III). Calibration of the low-resolution modules also used fainter standards (e.g., HD 42525, A0 V). Morris et al. (2003) provide more details about the calibration scheme. Decin et al. (2004) discuss the stars and synthetic spectra used for in-flight spectrophotometric calibration. We are also verifying the calibration using spectral templates generated as described by Cohen et al. (2003) and observations of additional standard stars.

TABLE 1
PROPERTIES OF THE IRS

Module	Array	Pixel Scale (arcsec)	Order	Slit Size (arcsec)	λ (μm)	$\lambda/\Delta\lambda$
Short-Low	Si : As	1.8	SL2	3.6 × 57	5.2–7.7[a]	80–128
			SL1	3.7 × 57	7.4–14.5	64–128
			"Blue" peak-up	56 × 80	13.3–18.7[b]	∼3
			"Red" peak-up	54 × 82	18.5–26.0[b]	∼3
Long-Low...........	Si : Sb	5.1	LL2	10.5 × 168	14.0–21.3[a]	80–128
			LL1	10.7 × 168	19.5–38.0	64–128
Short-High..........	Si : As	2.3	11–20	4.7 × 11.3	9.9–19.6	∼600
Long-High..........	Si : Sb	4.5	11–20	11.1 × 22.3	18.7–37.2	∼600

[a] The bonus orders cover 7.3–8.7 μm (SL) and 19.4–21.7 μm (LL).
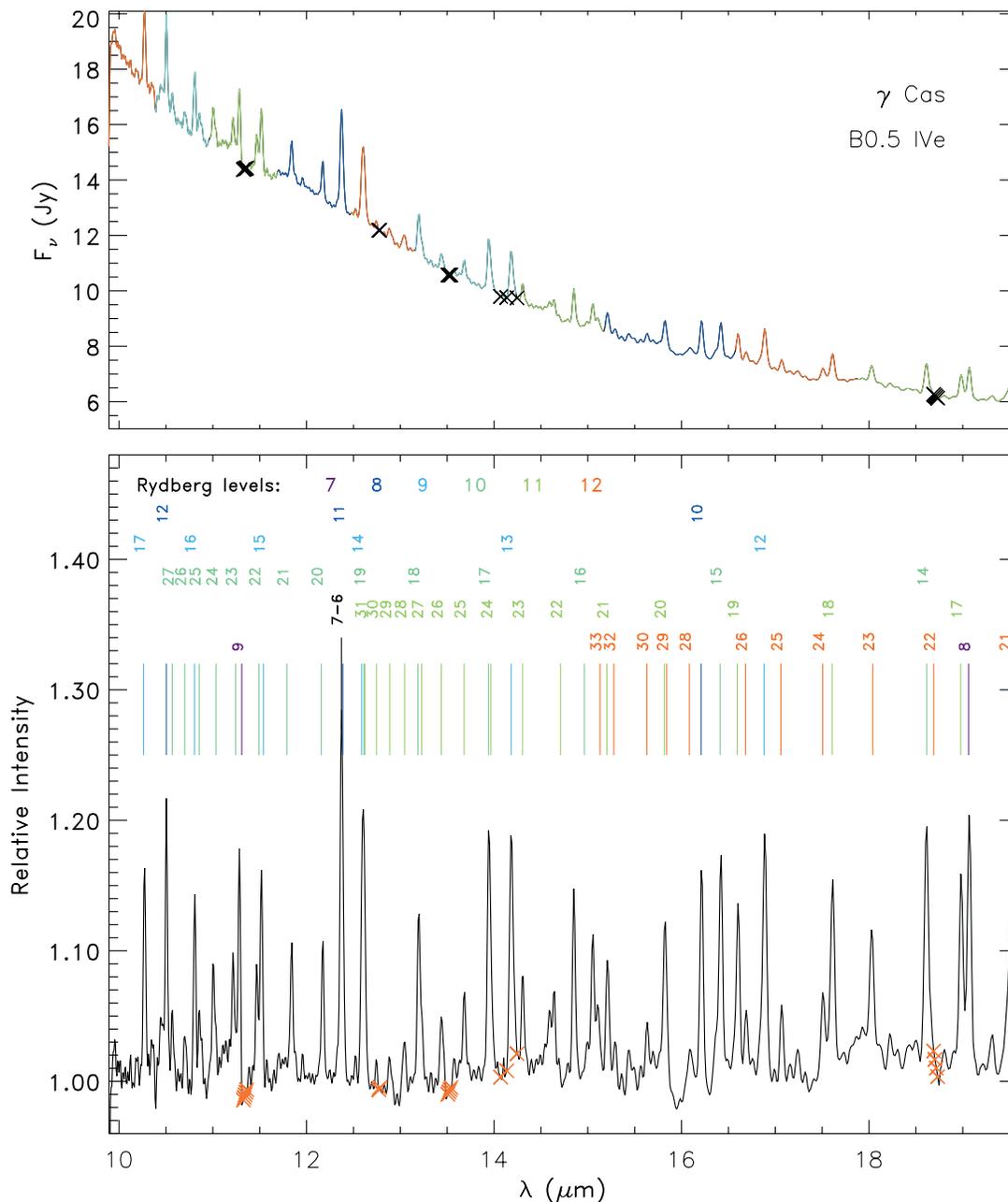[b] This is the full width at half-maximum of the filter.

F[IG]. 2.—SH spectrum of the Be star γ Cas. The lower panel shows a continuum-corrected spectrum with the identifications of the hydrogen recombination lines used to check the wavelength calibration of this module. The crosses mark the location of unusable wavelength elements.

The overlaps in wavelength coverage between the various modules and in orders within each module aid the internal cross-calibration of the IRS. These overlaps were also used to search for leaks in the order-sorting filters by observing "cold" and "hot" sources in two overlapping orders. In the case of the first-order filter for Long-Low (LL1), which had partially delaminated prior to launch, we used the combination of Uranus and Neptune as the cold sources and spectrophotometric standard stars as the hot sources. At this time the analysis limits any possible filter leak in LL1 to a maximum of $\sim$5% for a Rayleigh-Jeans spectrum. Further on-going efforts will refine this limit.

The third largest solar proton flare in the past 25 yr began on 2003 October 28, resulting in an integrated proton flux through the arrays of 1.9×10^9 protons cm^{-2}, equivalent to the 50 percentile dose expected during the first 2.6 yr of the mission. As a result, the sensitivity of $\sim$4% of the pixels in LH and $\sim$1% of the pixels in the other modules have been degraded. The degree of damage is consistent with the prelaunch damage experienced by nonflight arrays that were exposed to a beam of 40 MeV protons at the Harvard Cyclotron Facility. The IRS is more sensitive to damage than the other science instruments on board *Spitzer* because it is operating at lower background conditions where even a small increase in dark current has a significant effect.

The measured responsivity of the system in flight was on average 2 times better than the prelaunch model prediction. The detector noise measured in the unilluminated parts of the arrays are the same as measured prelaunch. Therefore, potentially in the limit of small signals the sensitivity is on

average 2 times better than the model predictions. Most of this increase is due to design margin, an assumed factor to account of errors and nonmodeled effects. The assumed margins were a factor of $\sqrt{2}$ for the short-wavelength modules and a factor of 2 for the long-wavelength modules.

Updated estimates of sensitivity are available in the current version of the SOM. The SSC provides a sensitivity calculator for the IRS known as SPEC-PET that includes detector noise, source shot noise, and background shot noise.[13] At the current time the sensitivity is limited by systematic effects, such as noise from the flat-field, fringing, and/or extraction edge effects, which are not included in the calculations of SPEC-PET. The observed sensitivities are approximately 3 times worse than would be achieved by the above responsivities and detector noise. It is anticipated that the realized sensitivities will improve as the system calibration improves.

4. USING THE IRS

4.1. *Spectroscopy*

The IRS currently has two modes of operation, the spectral "staring" and "mapping" modes. In both cases the target is acquired and then observed in a fixed sequence starting with SL2 (Short-Low second-order), SL1, SH, LL2, LL1, LH, skipping any unrequested slits.

The target acquisition method is selected by the observer. One may simply rely on the blind telescope pointing to point the slits to the specified position on the sky. A second option is to use the PCRS (Werner et al. 2004) to calculate the centroid of a reference star, use the offset between the star and the science target, and move the science target into the slit. A third and more accurate option is to use the IRS peak-up cameras to centroid on a 16 or 22 μm image of the science target or a reference star before commencing the requested spectroscopic observations (see § 4.2). Using the PCRS or IRS peak-up on a reference star requires accurate coordinates for both the offset star and the science target.

The IRS staring is the more basic mode of operation, and it results in observing the target at the 1/3 and 2/3 positions along the slit (its two nod positions), each with the integration time specified for that slit. The mapping mode steps the slit parallel and/or perpendicular to the slit according to the number and the size of the steps specified by the observer for each slit. The mapping mode does not perform the 1/3 and 2/3 nod observations that are automatically done in the staring mode.

Both the staring and mapping modes accept multiple target/position inputs, as long as all of the positions are within a 2° radius in the sky. Multiple targets are specified in a "cluster" list by either their (1) absolute positions, (2) right ascension and declination offsets, or (3) parallel/perpendicular slit offsets with respect to an absolute fiducial position. If using IRS in spectral mapping mode with cluster inputs, parallel/perpendicular slit offsets cannot be used. If the cluster specification is selected, all sources/offsets in the cluster are observed with the same slit before proceeding to the next slit. Use of the cluster specification, as opposed to repeating the same observation one source at a time, reduces the observatory overhead and can lead to substantial savings in total "wall clock" time.

The SOM describes the IRS observing modes and the various methods of target acquisition in more detail. In the

sections below, we concentrate on using the IRS peak-up cameras to place a target in the desired slit and describe how an observer can use the peak-up fields for imaging at 16 and 22 μm.

4.2. *IRS Peak-up*

The IRS SL module contains two peak-up imaging fields. Their field of view is $\sim55'' \times 80''$, with a scale of 1$\farcs$8 per pixel, and their bandpasses are centered at 16 and 22 μm for the "blue" and "red" camera, respectively (see Table 1). The IRS peak-up mode enables the placement of a source on a spectrographic slit or series of slits more accurately than just using blind pointing of the spacecraft alone. The telescope blind pointing has a positional accuracy of $\sim1''$ (1 σ rms radial). An on-board algorithm determines the centroid of the brightest source in the specified peak-up field and communicates the offsets required to accurately position the target in the requested slit to the spacecraft. As long as the coordinates of a target are accurate enough to place it on the peak-up imaging field and it is the brightest object in the field, the IRS will accurately offset to the selected slits. The peak-up images are supplied to the observers and can also be used scientifically if desired.

The allowed ranges of flux densities for blue and red peak-up point sources are $f_{\mathrm{blue}} = 0.8$–150 mJy and $f_{\mathrm{red}} = 1.4$–340 mJy, respectively. However, to avoid excessive integration times and a higher probability of failure, we recommend a flux of at least 2 mJy for the blue and 5 mJy for the red. The IRS peak-up algorithm has been optimized for point sources (and indeed this mode has been the most extensively tested and verified in-orbit), but an "extended source" mode is available for sources with diameters between 5$''$ and 20$''$ (e.g., comets). The allowed flux density range for extended sources, for either the blue or red mode, is $f_{\mathrm{ext}} = 15$–340 MJy sr^{-1}.

The observer can specify two peak-up accuracies: "High" and "Medium." In the simplest case, when peaking up on the science target itself, the first move to a slit after peak-up insures placement to within 0$\farcs$4 (1 σ rms radial) of the slit center for High Accuracy and 1$\farcs$0 for Medium Accuracy. The High Accuracy value is driven by the 5% radiometric accuracy requirement for the SH slit (4$\farcs$7 width). The IRS section of the SOM provides details on how these accuracy options apply to multiple slit positioning after peak-up (e.g., for targets in IRS cluster mode).

In the event that the science target cannot also serve as the peak-up target (e.g., if its flux is too low or too high), the "offset peak-up" mode gives the option of peaking-up using a nearby source. The observer is free to use any suitable source within 30$'$ of the science target, but the *Spitzer* planning tool (SPOT) also provides a list of recommended candidates. Note that this mode requires accurate coordinates for both the offset and science target. An IRS peak-up returns the image of the peak-up target.

The PCRS extends the IRS peak-up capability to optical point sources with visual magnitudes ranging between $m_V = 7$ and 10. The only mode for PCRS currently available provides pointing equivalent to the High Accuracy mode of the IRS. The PCRS peak-up does not produce or return an image.

4.3. *Imaging with the IRS Peak-up Arrays*

The peak-up fields in the SL module provide a means of obtaining images at 16 and 22 μm (5.4 and 7.5 μm FWHM, respectively). The 16 μm window in particular is interesting because the other cameras on *Spitzer* do not cover this

---

[13] See http://ssc.spitzer.caltech.edu/tools/specpet/.

wavelength region, and because this wavelength region was used by the *Infrared Space Observatory* (*ISO*) for most of its deep extragalactic surveys. Since these surveys probed the properties of galactic evolution only up to $z \sim 1$, IRS can provide the link between these past results and the new discoveries that will be made by *Spitzer* at $z > 2$.

Imaging with the IRS peak-up cameras has not been fully supported for the first year of operations, but the SSC will provide the ability to obtain large mosaics in a manner similar to IRAC (Fazio et al. 2004) before the end of 2005. However, an interim method called CHEAP (Cornell High-Efficiency Advanced Peak-up) has been used extensively to obtain mid-infrared images. CHEAP is based on an IRS SL staring observation and uses our knowledge of the offsets between the center of the peak-up windows and the SL slits in spacecraft coordinates, along with the standard two-position nodding along the slit, to place a source target in various positions on the two peak-up windows. The user may select any combination of exposure times and cycles of the SL to obtain an image. The data are processed by the standard SSC pipeline as though they are standard SL spectroscopic observations. The software that combines and calibrates the produced images is already available.

As an example, taking a CHEAP image using a standard 60 s SL staring exposure will produce two images at 16 and 22 μm with an rms noise of $\sim$30 μJy in only $\sim$720 s of total time. It is interesting to note that the rms noise of the *ISO* observations of the Hubble Deep Field (HDF) was just $\sim$13 μJy at 15 μm and that the faintest source detected in the HDF at 15 μm was 50% brighter than the sensitivity in the above example (Aussel et al. 1999). The use of CHEAP to obtain 16 and 22 μm images of a sample of high-redshift ($z > 1.5$) submillimeter galaxies is presented by Charmandaris et al. (2004), and the first 16 μm imaging of a Lyman Break Galaxy at $z = 2.79$ is discussed by Teplitz et al. (2004).

4.4. *Planning IRS Observations*

A number of issues should be considered in the design of spectroscopic observations using IRS. These are addressed in detail in the SOM, but we briefly mention a few of the more important ones in this section.

Although the infrared background is fainter than the ground-based background by a factor of 10^6, it may still be necessary to take an "off-source" measurement of the background. The low-resolution modules do this automatically in the sense that both subslits are exposed at the same time so the spectrum from the "off" slit can be subtracted from the "on" slit to remove the background. Alternately, the low-resolution slits are long enough to do the background subtraction on the slit itself. However, the high-resolution slits are too short to subtract the background by differencing the nod positions. If the continuum level is important, off-source integrations using the same module are required for the purpose of background subtraction. SPOT provides an estimate of the background that is helpful in planning for background subtraction. As a general rule, the observers should use the low-resolution modules to measure continuum and broadband features, and the high-resolution modules to measure unresolved lines.

The peak-up system works extremely well over its range of parameters. However, the observer needs to carefully check that the flux of the peak-up candidate falls within the specified limits of the cameras and correctly enter it into SPOT. Furthermore, as already mentioned in § 4.2 the candidate must be the brightest object within $\sim$120$''$, to ensure that it will be the

one selected by the peak-up algorithm. There have been several peak-up failures due to violations of one or the other of the above requirements.

Observing with *Spitzer* is unlike most ground-based infrared observing. On the ground the background signal overwhelms the source by many orders of magnitude. Therefore, the system noise is set by the shot noise from the background. On *Spitzer*, the noise (N) is dominated by detector noise for small signals (S), so N $\sim$ constant. However, as the signal level increases the shot noise in the signal eventually dominates: N $\propto$ S$^{1/2}$. At the highest signal levels fixed pattern noise (flat-fielding errors, etc.) are dominant and consequently N $\propto$ S. At the present time it appears that the flat-fielding term is 1% to 2%, effectively limiting the maximum S/N to $\sim$50–100. Similarly, at very low signals the flat-field uncertainty limits our 1 σ detection to $\sim$0.3 mJy at 16 μm for low backgrounds (see Higdon et al. 2004a). The online S/N estimator includes all but this last term.

5. PIPELINE DATA PROCESSING

As described in detail in the SOM, IRS observations, either in DCS or Raw mode, are stored as FITS files of what is called a Data Collection Event (DCE). A DCE contains all the data obtained by an IRS module since the most recent destructive read. The IRS Science Pipeline at the SSC treats each DCE independently. The processing of DCS data, such as those collected during an IRS peak-up, by the pipeline is minimal and all processing is performed on board the spacecraft. However, for data obtained in Raw mode the pipeline removes basic instrumental signatures and corrects for variations in spectral response within and between spectral orders. A number of these steps, such as corrections/checks for saturation, cosmic rays, dark current subtraction, as well as linearization, are performed in the cube level prior to fitting a slope to the sampled up the detector charge integration ramp. Others, such as correction for drifts in the dark current, and stray light or crosstalk between the orders are applied once the slope image has been created.

The IRS array data supplied in FITS files to the observer are organized into four categories: Engineering Pipeline Data, Basic Calibrated Data (BCD), Browse-Quality Data (BQD), and Calibration Data. Additional files are also available of the masks used in the pipeline processing as well as processing log and quality assurance files. The Engineering Pipeline data consist of the raw detector sample images, with some descriptive information in the FITS file headers. The BCD files are the fundamental basis for science analysis, with the primary product being a two-dimensional slope image of each DCE in units of electrons s^{-1} pixel^{-1}, accompanied by a header containing the essential programmatic information and the processing, calibration, and pointing history. Additional BCD data files include uncertainty images that accompany each slope image and various intermediate images that do not have all of the pipeline processing corrections applied. The BCD also include co-added image data for those observations with more than one ramp at a sky location. It is expected that the BCD files will be used by the IRS observers as the standard data input for subsequent publishable science data analysis. As an example, in a standard IRS staring observation in which the observer has requested three cycles of 30 s integrations on a science target with the SH module will result in six DCEs in Raw mode. The Engineering Data pipeline will process the data, which will have the form of six data cubes (three integration cycles at each of the two nod positions along

the slit), each 128×128 pixels $\times 16$ detector reads in size. The BCD pipeline will produce six 128×128 BCD slope images as well as two 128×128 co-added slope images. The Calibration Data include measurements of standard calibration objects and can be used with the BCD to further refine the quality of the science data.

The BQD is designed to provide the observer with an early look at spectra extracted from two-dimensional BCD images of point sources. In general, the BQD spectra are designed to convey the richness of the observed data and in some cases may be of publishable quality. To extract spectra from each individual BCD image, the post-BCD pipeline first applies a search algorithm to trace the spectrum in the two-dimensional 128×128 pixel images. Extraction is performed using an aperture that follows the linear expansion of the point spread function (PSF) with wavelength. All spectra are extracted as point sources, and no sky background is subtracted before the extraction is made (see discussion in § 4.1 on how this may affect the extracted spectrum). The spectra are then photometrically calibrated (in Jy) to remove the effects of truncation of the PSF by the slit aperture and high-order systematic residuals from flat-fielding.

Most pipeline operations are now routine, but the need to characterize the performance of the instrument in-orbit has led to numerous modifications to the algorithms and adjustments to parameters. Most important are ongoing efforts to refine the detection and mitigation of latencies and cosmic-ray hits, correct for stray light between the echelle orders, and remove stray light in the SL module originating from the peak-up apertures. Extraction methods and the final spectrophotometric calibration of the spectra are also very sensitive to the pixelation of PSF at each wavelength, and as a result both the extraction and calibration will require some fine-tuning as a result of what has been learned from in-flight measurements. A detailed user's guide to the SSC pipeline and its products is in preparation.

6. SPECTROSCOPY MODELING, ANALYSIS AND REDUCTION TOOL

The IRS Spectroscopy Modeling, Analysis, and Reduction Tool (SMART) is an IDL software package used to reduce and analyze IRS data from the four modules and the two peak-up arrays.[14] SMART is designed to operate on the Basic Calibrated Data (BCD) delivered by the SSC pipeline and can be run both interactively and in batch mode. It provides a suite of quick-look routines that enable observers to assess the quality of their data.

SMART extracts spectra from either individual or co-added BCDs, and these can be weighted by a pixel mask, which characterizes the noise in the data. The extraction routines include column extraction of a point source scaled to the instrumental PSF, fixed-aperture extraction for extended sources and a weighted Gaussian extraction for point sources.

Several options are available to optimize the sky subtraction. The spectra from the individual modules can be combined to produce a single spectrum from 5 to 38 μm. Spectral analysis, including line, blackbody, template and zodiacal light fitting, photometry, defringing, and dereddening, are also available. The spectral analysis package is based on the *ISO* Spectral Analysis Package (ISAP; Sturm et al. 1998). SMART
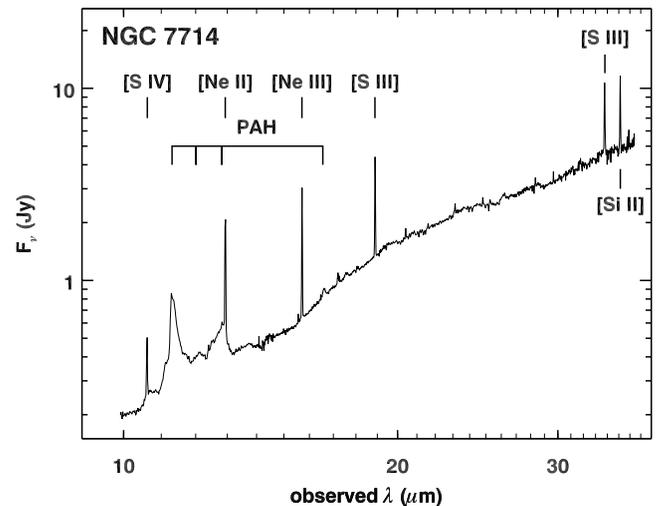

Fɪɢ. 3.—High-resolution spectrum of the starburst galaxy NGC 7714 (using both SH and LH) with the detected features marked (shifted for $z = 0.0093$). This spectrum was obtained with 240 s of integration in SH and LH (each). Brandl et al. (2004) describe these observations in more detail.

includes packages developed by the *Spitzer* Legacy teams. The c2d team provided a number of defringing tools while the FEPS team has contributed IDP3, an image analysis software package originally developed for the NICMOS instrument of the *Hubble Space Telescope*.

Higdon et al. (2004b) provide more details about the SMART package. It will become publicly available in 2004 September.

7. SAMPLE RESULTS

The articles in this special *Spitzer* issue provide many examples of the quality of the spectra from the IRS. In addition to the spectrum of γ Cas in Figure 2, we show examples of one low-resolution spectrum and one high-resolution spectrum, both of galaxies. All data presented have been processed and extracted from individual DCEs using the IRS pipeline at the SSC. Figure 3 presents a spectrum of NGC 7714 using
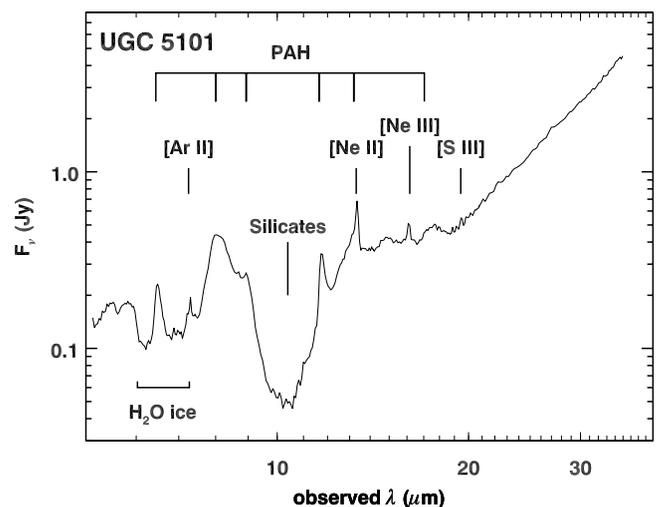

Fɪɢ. 4.—Low-resolution spectrum of UGC 5101 (using both SL and LL), showing several strong bands from PAHs, dust, and ice along with atomic emission lines (redshifted for $z = 0.039$). The integration time was 12 s in each SL subslit and 28 s in each LL subslit (total 80 s). Armus et al. (2004) discuss this spectrum more completely.

---

[14] Cornell maintains information on their Web site for SMART and updates it regularly. See http://isc.astro.cornell.edu/smart.

SH and LH (240 s integration each). Brandl et al. (2004) describe this spectrum in more detail, but one can immediately note the many forbidden lines and dust features present. Figure 4 presents the spectrum of UGC 5101 obtained using the low-resolution modules. The integration times were 12 s in each SL subslit and 28 s in each LL subslit, and this was sufficient to show a rich spectrum with gas, dust, and ice features. See Armus et al. (2004) for more information on this spectrum.

8. CONCLUSION

The IRS is a major step forward in speed and sensitivity. It clearly enables the extension of infrared spectroscopy to a very large number of extragalactic sources. The designed spectral resolution is well matched to the expected line widths from these objects. The IRS also allows mid-infrared spectroscopy of objects such as brown dwarfs, individual stars in neighboring galaxies, and a wide variety of other sources previously difficult or impossible to study spectroscopically in the mid-infrared. This description of the IRS gives the potential observer a brief review of its design, its capabilities, and how to use it. Now it is up to the astronomical community to fully exploit what the IRS can do.

REFERENCES

Armus, L., et al. 2004, ApJS, 154, 178
Aussel, H., Cesarsky, C. J., Elbaz, D., & Starck, J. L. 1999, A&A, 342, 313
Brandl, B. R., et al. 2004, ApJS, 154, 188
Charmandaris, V., et al. 2004, ApJS, 154, 142
Cohen, M., Megeath, T. G., Hammersley, P. L., Martin-Luis, F., & Stauffer, J. 2003, AJ, 125, 2645
Decin, L., Morris, P. W., Appleton, P. N., Charmandaris, V., & Armus, L. 2004, ApJS, 154, 408
Fazio, G., et al. 2004, ApJS, 154, 10
Higdon, S. J. U., et al. 2004a, ApJS, 154, 174
———. 2004b, PASP, submitted
Houck, J. R., Roellig, T. L., van Cleve, J., Brandl, B. R., & Uchida, K. I. 2000, SPIE, 4131, 70

Morris, P. W., Charmandaris, V., Herter, T., Armus, L., Houck, J. R., & Sloan, G. C. 2003, in The Calibration Legacy of the ISO Mission (ESA SP-481; Noordwijk: ESA), 113
Smith, J. D. T., & Houck, J. R. 2001, AJ, 121, 2115
Sturm, E., et al. 1998, in ASP Conf. Ser. 145, Astronomical Data Analysis Software and Systems VII, ed. R. Albrecht, R. N. Hook, & H. A. Bushouse (San Francisco: ASP), 161
Teplitz, H., I., et al. 2004, ApJS, 154, 103
van Cleve, J., et al. 1998, PASP, 110, 1479
Werner, M. W., et al. 2004, ApJS, 154, 1